Classification
Physics Abstracts
61.30J — 61.30G — 47.30

Ising-Bloch transition in a nematic liquid crystal

J.M Gilli (*), M. Morabito and T. Frisch

INLN (**), 1361 Route des Lucioles, 06560 Valbonne, France

(Received 12 July 1993, received in final form 21 September 1993, accepted 8 November 1993)

Résumé. — Nous avons étudié, sur une lamelle nématique, avec un ancrage homéotrope, l'effet d'un champ magnétique, H, parallèle aux lames, associé à un champ électrique, E, parallèle à ces dernières ($\epsilon_a < 0$, $\chi_a > 0$). Le champ magnétique peut être fixe ou tournant à une vitesse ω autour d'un axe perpendiculaire aux lames. Le principal effet étudié ici concerne une transition Ising-Bloch des parois, observée dans les espaces de paramètres (H^2, E^2) ou (H^2, ω). Ce dernier cas correspond à l'observation expérimentale récemment réalisée à l'Université de Brandeis [1]. Certains de ces résultats sont interprétés à l'aide d'un modèle à la Ginzburg-Landau directement déduit de l'expression de Oseen-Zocher-Frank de l'élasticité des nématiques. Les textures constituées de spirales obtenues dans le cas dynamique sont probablement l'un des premiers analogues physiques simples des spirales chimiques et biologiques étudiées dans le domaine des milieux excitables.

Abstract. — We consider a nematic slab with homeotropic anchoring and investigate the effect of a magnetic field, H, parallel to the plates and an electric field, E, perpendicular to them ($\epsilon_a < 0$, $\chi_a > 0$). The magnetic field is either fixed, or rotating at a frequency ω around an axis perpendicular to the plate. The main effect consists in an Ising-Bloch transition of the walls observed either in the (H^2, E^2) or (H^2, ω) parameter space. The latter case corresponds to the experimental observation recently made at Brandeis University [1]. Some of these results are understood within the framework of a Ginzburg-Landau model, directly derived from the Oseen-Zocher-Frank expression for nematic elasticity, which accounts for the main static and dynamic experimental phenomena observed. The spiral shaped textures obtained in the dynamic case probably represent one of the first simple physical analogs of the chemical and biological phenomena observed in excitable media.

(*) also at URA CNRS 190, UNSA, Faculté des Sciences, 06108 Nice Cedex 2, France.
(**) UMR CNRS 129.

1. Introduction.

In a recent article, Migler and Meyer [1], give a sophisticated version of the experiment of reference [2]. In the presence of a magnetic field, H, rotating around an axis perpendicular to the glass plates which form a nematic liquid crystal cell, a structural transformation of the Brochard-Leger walls into pure dynamical splay-bend ones was observed, when the rotation frequency, ω, was increased above a field dependent threshold. As described in another paper [3], we have developed a Ginzburg-Landau (G-L) dynamical model derived from the Frank nematic elasticity, which accounts for the main characteristics of the (H^2,ω) experimental phase diagram. In [3] we have demonstrated the usefulness of a two-dimensional order parameter $A(x,y)$ defined by $n_x + in_y = A(x,y)\cos(\pi z/d)$ where d is the sample thickness. A is proportional to the projection of the nematic director, $\mathbf{n}$, on the (x,y) plane. On the basis of this model, the wall transformation observed by the Brandeis group [1], can be understood as an Ising-Bloch (I-B) transition of the type predicted theoretically [4] for a magnetic 2D medium in a dissipative, out-of-equilibrium situation. As described in [4], the order parameter vanishes at the center of the Ising-wall, while it does not at the center of the Bloch wall. In the following, we refer to the Brochard-Leger (B-L) wall, (observed in the bend geometry of the Freedericksz transition [5]) as an Ising-wall. Indeed, according to the definition of our order parameter, at the center of the Brochard-Leger wall, the director points towards the $\hat{z}$ direction and therefore $A = 0$. On the other hand we refer to the dynamical soliton observed in [1] as a Bloch wall because at the center, the director is not perpendicular to the glass plate and therefore $A \neq 0$. We use a different version of the Brandeis experiment, in which an AC electric field, E, perpendicular to the glass plates is applied simultaneously with a magnetic field, H, parallel to the plates. The rotating magnetic field is produced by the use of rotating permanent magnets and the liquid crystal sample remains fixed in the laboratory frame. Here, we mainly describe the situation at thermodynamic equilibrium, corresponding to an $\omega = 0$ situation, and, in agreement with the model, observe the first unquestionable experimental evidence of the static I-B transition in the (H^2, E^2) parameter space. This transition, induced by a temperature variation, was theoretically predicted [6, 7] in the neighborhood of the Curie point of a magnetic system.

This transition is also observed when the walls are curved and closed in the form of loops: in this case the curvature effect leads to the reproducible observation of a particular "four defect" symmetry breaking situation. This is comparable, in its main aspects, to the situation observed in reference [1a] in the case of an out-of-equilibrium, rotating field experiment.

2. Experimental set-up.

The experiments described in the following (Fig. 1) have been carried out in the optical path (direction z) of an Olympus polarizing microscope. A simple DC motor with variable reduction ratio rotates a plate supporting two small permanent Nd-Fe-B magnets which produce a magnetic induction of 0.7 tesla between the poles. In the preliminary experiments, the samples stand in the upper part of the magnet in a region of curved field lines: this situation and the opposed direction of the Hz component in the pole vicinity suppress the degeneracy of the Freedericksz magnetic transition and a S-B, B-L straight wall perpendicular to H is spontaneously obtained in the central region of our samples (Photo. 1a).

An AC electric field is applied perpendicular to the plate by the use of evaporated ITO (Indium Tin Oxide) on the conducting glass plates. Homeotropic anchoring is achieved by treating our glass plates with lecithin. A 1000Hz AC electric field was generally used to avoid space charge phenomena. The thickness, d, of the sample was in general about 75 μm.

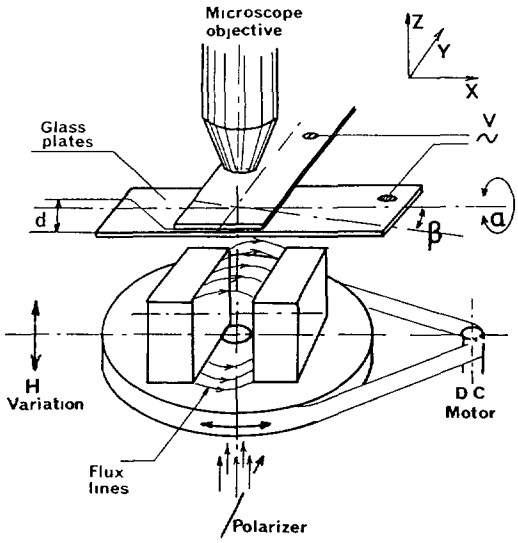

Fig. 1. — Scheme of the experiment. The ITO treated glass plates filled with homeotropic nematic are placed in the air-gap upper region of a high flux permanent magnet allowed to rotate around the polarizing microscope axis. The magnetic field is varied by the adjustment of the distance between the nematic slab and the upper surface of the magnets. An AC electric field perpendicular to the plate can be applied simultaneously.

The liquid crystal used is the well-known MBBA, nematic at room temperature, which possesses a sufficiently high $\zeta_a = 10^{-7}$ Emu cgs·g^{-1} and a negative $\epsilon_a = -0.7$. As those given in the literature [8], the elastic constants are anisotropic: $K_1 = 6 \times 10^{-7}$ dynes, $K_2 = 4 \times 10^{-7}$dynes, $K_3 = 7.5 \times 10^{-7}$dynes around 25 °C.

3. Experimental results.

3.1 The static case $\omega = 0$.

3.1.1 *Ising-Bloch transition of a straight wall.* — When the strength of the stationary magnetic field is increased, the straight wall, spontaneously observed in the particular geometry of our experiment, decreases its width but always exhibits a black homeotropic region easily observed between crossed polarizers in its middle part (Photo. 1a): this is Splay-Bend B-L wall [5]. Remaining on an intermediate value of H, and increasing now the electric field, this wall undergoes a transformation at a particular threshold E_1 (Photos. 1b and c). If the field is increased slowly, this transformation operates *via* the progression of an interface coming from one of the sample limits, separating the disappearing Ising B-L region from a new appearing structure. If the field is increased quickly, this transformation starts from different parts of the wall, and defects are obtained along it when equilibrium is reached. As developed in the theoretical part of this paper, this transformation corresponds to an I-B second order transition, the electric free energy of the middle part of the wall with n parallel to z becomes prohibitive when E increases and the director reorients toward the (x, y) plane. The experimental situations corresponding to the Ising or Bloch character of the wall are easily distinguished when the wall is parallel to the polarisation direction: the Ising wall remains extinguished whereas

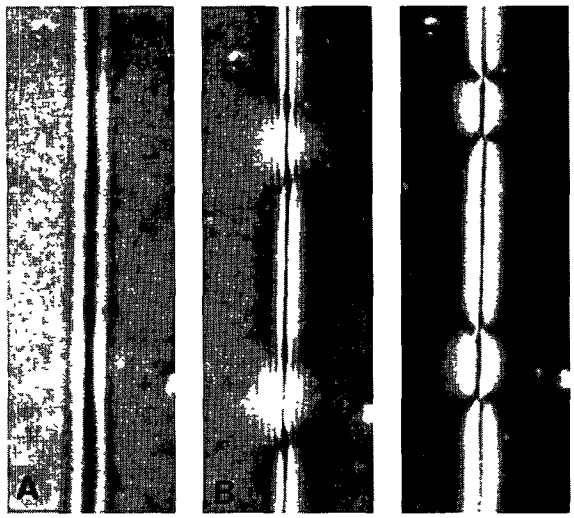

Photo. 1. — The I-B transition of a straight splay-bend wall parallel to the polarizer. a) the Ising wall just starts its transformation ($E = E_1$). b), c) The $E > E_1$ situation leads to the formation of topological defects, two groups of +1 −1 are visible in the upper and lower parts of the photographs.

the Bloch wall is strongly illuminated, except for a thin black line in the middle part of the wall. This fact is related to an in-plane rotation of the projected director component A. We obtained the preliminary experimental points of figure 2, corresponding to the onset of light in the immediate neighborhood of the wall when the voltage is slowly increased (1 V/1000 s).

This procedure gives only poor accuracy in the low magnetic field domain due to the diverging transition times and to the low intensity of light but it proves nevertheless a rather good agreement with the model presented below.

The introduction of a waveplate between the two polarizers, with its principal axes oriented at $\pi/4$ relative to their directions makes it possible to distinguish the two different tilting directions of A from the initial magnetic field one.

The defects observed along these Bloch walls are non-singular $|s| = 1$ disclinations, with +1 and −1 topological charges alternating along the wall. The four extinction lines of the +1 defects rotate in the same direction as the polarizers and are easily distinguished from the counter-rotating lines of the −1 defects. Moreover, the +1 looks like a rounded core in contrast to the −1, which appears as a rhombus. The defect formation is easily understood from the two equiprobable possible tilting directions at the I-B transition (Fig. 3c): they are formed at the junction of two different tilting direction wall domains.

An interesting additional experimental observation concerning the +1 defect obtained along the wall is illustrated in photograph 2. After a few minutes, the initially straight wall of photograph 1c undergoes a deformation: the extinction lines around the +1 defect take the shape of a spiral and the wall represents an inflection point. If we relax the wall to its Ising form, this curvature induced by the presence of positive disclinations is maintained for a while before the effect of the surface tension smoothly deletes it. This effect is probably related to the instability of the splay core of the initial +1 defect relative to a double twist one. Since this experiment is performed with a nematic non-chiral liquid crystal, the two opposite twist situations are equally probable, corresponding to both possible wall rotations around the defect. Concerning this distortion, it is not yet clear if it starts at the onset of the S-B, I-B transition

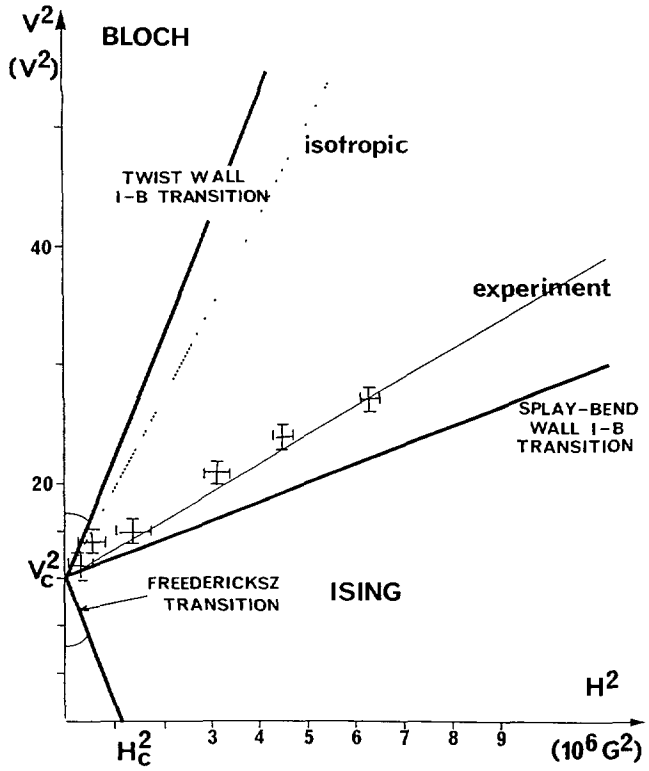

Fig. 2. — The experimental and theoretical phase diagram of the Ising-Bloch variational transition in (H^2, E^2) parameter space. The agreement is rather good between the preliminary measurements made on the splay-bend initial Ising wall and the theoretical bifurcation. The theoretical transition line given in the isotropic elasticity case corresponds to the condition $\gamma = \mu/3$ in the model.

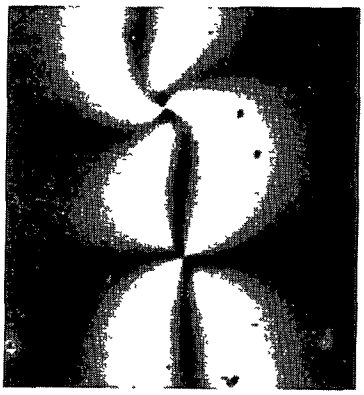

Photo. 2. — After a few minutes, the +1 formation (upper defect) leads to the spiral shape of the extinction lines and to a curvature induced effect on the wall. This is probably explained by the instability of the initial all splay core of the +1.

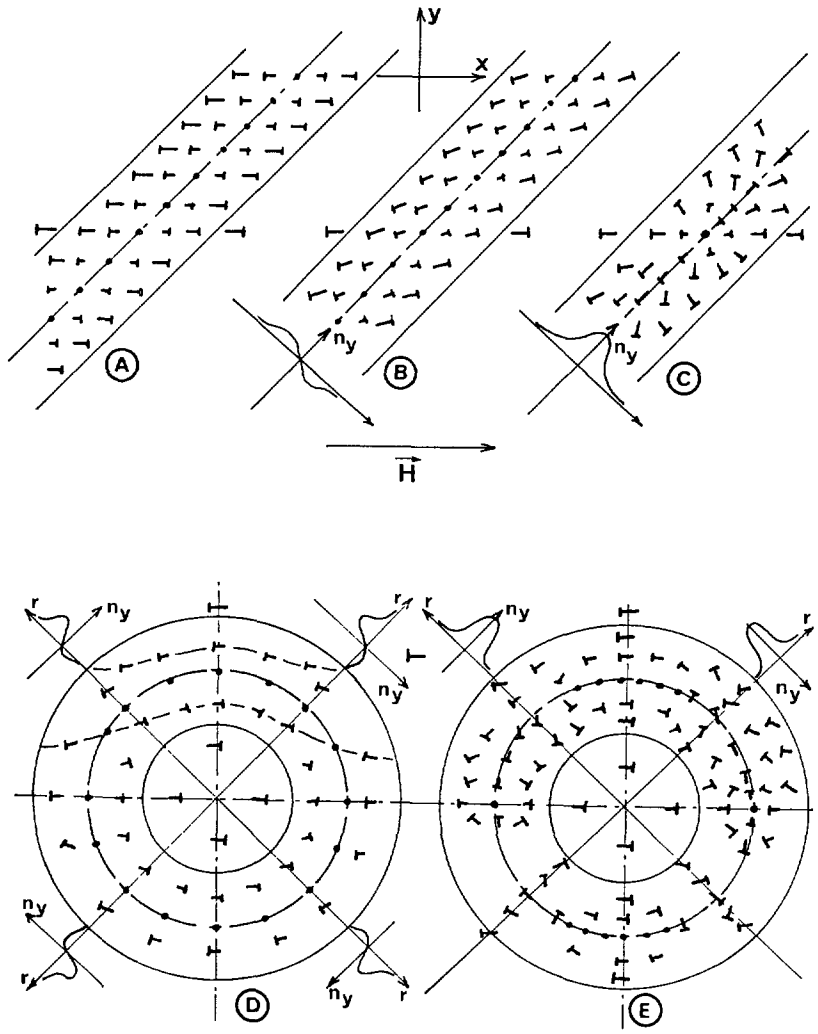

Fig. 3. — The looped wall transformation with the nail convention. a) An Ising wall at 45° of the pure S-B or twist situation in the isotropic elasticity case. b) Same as a) but in a more realistic anisotropic situation. c) The I-B transition is degenerated, and both tilt orientations are equally probable ($n_y > 0$ or $n_y < 0$), allowing for the trapping of disclinations (here $a + 1$) along the wall. d) The Ising loop in the anisotropic case: due to the curvature effect the n_y component is no longer symmetric relative to the wall's center in the oblique regions. e) From this last fact, the degeneracy of the transition is removed in this region and, associated with the change of sign of n_y in the four quadrants of the loop, four defects remain trapped.

or if it constitutes an independent bifurcation.

It is important to remark here that this observation of the threshold-second order I-B transition under the experimental conditions previously described requires a good parallelism of the plates relative to the upper surface of the magnets.

Indeed, the presence of an angle α (Fig. 1) of the initial B-L wall relative to this surface rules out the degeneracy of the tilting direction (this is achieved in the same way as the classical magnetic bend geometry Freedericksz transition). In this case, a vanishingly low electric field confers a Bloch character to the wall, and no defects are observable along it.

The other possible angle β of the plate has less influence on the phenomena described here (the wall is progressively moved away from the optical axis of the microscope). On the contrary, as mentioned later and developed in reference [9], the presence of α or β angle takes a great importance in the case of the physical dynamical process involving archimedian spirals.

3.1.2 *Ising-Bloch transition of a looped wall.* — As mentioned in reference [1] and described below, the out-of-equilibrium behavior which occurs when the magnetic field is rotated, gives us a useful way to obtain "dynamic solitons" loops. In our observation field, these loops are constituted by Bloch walls devoid of defects. If we come back to the static magnetic field situation in the presence of an AC electric field, E, a characteristic behavior of these loops is obtained by a simple variation of E. Starting from the Bloch loop without defects, the decrease of E leads to the Bloch-Ising transformation and a slow shrinking of the Ising loop is observed. The Ising loop takes an elliptical shape related to the anisotropy of the elastic constants, with the major axis directed along the H direction [5]. For small diameter-high curvature loops, a new increase of E now leads to the reproducible particular behavior observed in photomicrograph 3: if E is slowly increased, at a particular threshold, E_1, the formation of two defects of the -1 type is first observed on two opposite points of the loop, the direction joining these points being that of the magnetic field. An elongated structure appears simultaneously in the perpendicular direction corresponding to the minor axis of the ellipse. These two regions progressively decrease their lengths as E increases and, at a second threshold, E_2, give rise to two $+1$ disclinations. As described in the following, this phenomenon, also observed in a more complex out-of-equilibrium situation (1a), is related not only to the anisotropy of elastic constants i.e. the different elastic energy of splay-bend or twist Ising wall regions, but also to the curvature of the looped walls. The two different I-B transition thresholds of the splay-bend (E_1) and twist (E_2) regions explain the successive formation of the -1 and $+1$ defects.

3.2 THE ROTATING CASE $\omega \neq 0$. — Let us rotate the magnetic field, H, around the z axis, starting from an Ising domain ($E < E_1$) of the (V^2, H^2) phase diagram where $V = \mathrm{d}E$.

At low ω, the straight Ising, B-L wall which is initially present in the middle of the optical field does not follow the rotation of the magnets. This is true only in the central region of our sample in which the field lines are parallel to the glass plate. In the peripheral regions, where the field possesses a non-negligible component along z, the curved magnetic lines cause the Ising wall to reorient and to follow the field.

Restricting ourselves to the central region of the sample, a progressive increase of ω leads to the same transformation previously described in the static case, and associated with the I-B transition. This transformation of the wall in a rotating magnetic field has been described as a static-to-dynamic soliton transition in reference [1]. The wall presents a high contrast aspect in the Bloch regime and undergoes now a transverse drift. Moreover, the axial symmetry of our experimental geometry leads to the reproducible formation of a $+1$ disclination on the wall, on the rotation axis of H. The transverse drift direction is reversed when the disclination is crossed along the wall and the latter consequently takes the shape of a spiral (Photo. 4). In this photograph, it is important to note the asymmetry of the arm related to its transverse drift: the extinction in the front of the wall is rather sharp, contrary to the back part extinction which is spread on a larger scale.

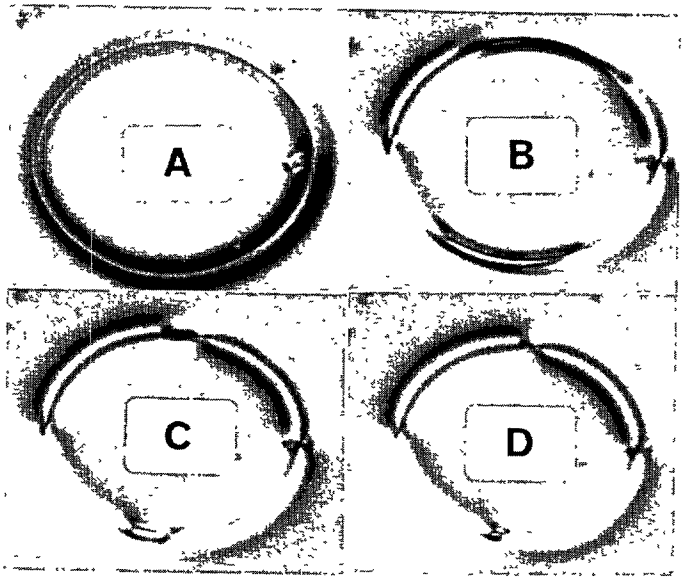

Photo. 3. — The looped wall transformation in a horizontal magnetic field. a) The initial elliptical Ising ring. b), c) when $E_2 > E > E_1$ two -1 defects are obtained along the major axis of the ellipse and an elongated region (in the vertical domains) progressively shrinks as E is increased. d) For $E > E_2$, two $+1$ defects are formed.

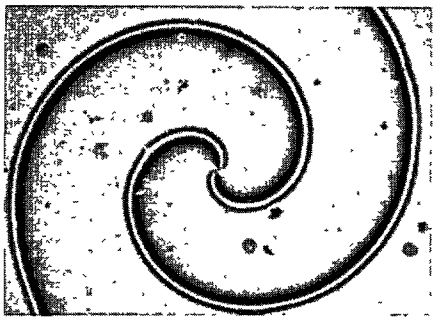

Photo. 4. — When the field H is rotated, starting from the initial Ising splay bend wall, and if the frequency ω is between the lowest ω_{I-B} threshold of the I-B, S-B transition and the asynchronous one, a $+1$ disclination is formed on the microscope axis and the wall forms an Archimedian spiral. The drift leads to an asymmetry of the spatial rotation of n when crossing the wall as seen by the different shapes of the two extinction lines.

The presence of non-zero angles β or α allows in fact for a progressive appearance of the asymmetry of stability of both the initially possible homogeneous domains, thus giving rise to the formation of single-arm Archimedian spirals, rotating around a topological defect of $|1|$ character (Photo. 5). These "single arm" spirals seem to be one of the first physical analogues [9] of the chemical [10], and biological [11] spirals, extensively studied in the area of excitable media.

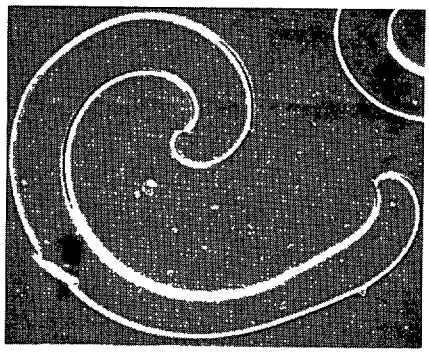

Photo. 5. — When the angles α or β are increased from zero, one of the two initially equivalent homogeneous domains becomes unfavorable and 360° walls appear, in the form of one arm Archimedian spirals rotating with different pitches and speeds around the initial +1 and -1 defects.

4. The model.

As theoretically predicted in reference [4] for the case of ferromagnetic media and developed in associated theoretical papers [3] for the nematic case, the experiment can be described within the framework of a G-L approach ([1]). Our theoretical approach assumes that the director is only weakly tilted from the z axis. This condition is satisfied only in the vicinity of the Freedericksz transition, a condition which is not fulfilled in [1]. Furthermore, the magnetic field is considered as a small perturbation of the main electrical field. The dynamical equation for the director $\mathbf{n}$ reads

$$\gamma_1 \mathbf{n} \times \mathbf{n}_t = -\mathbf{n} \times \frac{\delta F}{\partial \mathbf{n}} \tag{1}$$

where γ_1 is the rotational viscosity and the Frank free energy reads

$$\begin{aligned} F &= \frac{1}{2}\int \mathrm{d}v(K_1(\nabla \cdot \mathbf{n})^2 + K_2(\mathbf{n} \cdot \nabla \times \mathbf{n})^2 + K_3(\mathbf{n} \times \nabla \times \mathbf{n})^2 \\ &\quad -\chi_a(\mathbf{H} \cdot \mathbf{n})^2 - \Delta\epsilon(\mathbf{E} \cdot \mathbf{n})^2) \end{aligned}$$

where $\mathbf{H} = H\hat{x}$, $\mathbf{E} = E\hat{z}$, and K_1, K_2, K_3 are the elastic constants. The linear stability analysis of equation (1) shows that when $\chi_a H^2 - \epsilon_a E^2 - (k_3\pi/d^2) > 0$, the homeotropic state corresponding to $\mathbf{n} = \hat{z}$ becomes unstable (d is the thickness of the sample).

It is then natural to make a vertical Fourier expansion in which we keep only the first unstable mode. It can be easily shown that in the vicinity of the Freedericksz transition the higher order vertical distortion modes are damped and therefore follow adiabatically the first unstable mode. For an order parameter, let us take $A(x,y) = X(x,y) + iY(x,y)$, which measures the deviation from the homeotropic states, where $X(x,y)$ and $Y(x,y)$ are defined by

$$n_x = X(x,y)\cos(\pi z/d),$$

$$n_y = Y(x,y)\cos(\pi z/d),$$

$$n_z = 1 - (n_x^2 + n_y^2)/2$$

([1]) This model was developed in collaboration with S. Rica and P. Coullet [3].

and d is the thickness of the sample. Direct replacement of this *Ansatz* into equation (1) leads after some algebra to

$$\gamma_1 X_t = (\mu+\gamma)X + K_2\nabla^2 X + (K_1-K_2)(X_{xx}+Y_{xy}) - a(X^2+Y^2)X \quad (2)$$

$$\gamma_1 Y_t = (\mu-\gamma)Y + K_2\nabla^2 Y + (K_1-K_2)(X_{xy}+Y_{yy}) - a(X^2+Y^2)Y \quad (3)$$

where $\mu = \frac{\chi_a}{2}H^2 - \epsilon_a E^2 - K_3\frac{\pi^2}{d^2}$, $\gamma = \frac{\chi_a}{2}H^2$, $a = \frac{1}{2}(K_1 - \frac{3}{2}K_3)\frac{\pi^2}{d^2} - \frac{3}{4}\epsilon_a E^2$, $\nabla^2 = \partial_{xx} + \partial_{yy}$.

Setting $A(x,y) = X(x,y) + iY(x,y)$ in these last equations we obtain

$$\gamma_1 A_t = \mu A + \gamma\bar{A}e^{-2i\omega t} + \frac{K_1+K_2}{2}\nabla^2 A + \frac{K_1-K_2}{2}\bar{A}_{\eta\eta} - a|A|^2 A \quad (4)$$

where $\partial_\eta = \partial_x + i\partial_y$, and $\bar{A}$ stands for the complex conjugate.
This equation is very similar to the one studied in (4) except for the term $\bar{A}_{\eta\eta}$ which is proportional to $K_1 - K_2$. When $K_1 = K_2$, equation (4) reduces to the model used in (4) in which it is shown that an Ising wall looses stability toward a Bloch wall when $\gamma < \mu/3$.

The term in $\bar{A}_{\eta\eta}$ which conveys the anisotropy of elasticity of the nematic liquid crystal is not present in the Heisenberg ferromagnetism. In this case, rotation of the spins does not change the Heisenberg free energy while in the nematic phase a rotation of the molecules changes the Frank free energy. As a consequence, the dynamical equation (4) should not be invariant under the transformation $A \to A^{i\phi}$ which conveys a rotation of the molecules by an angle ϕ around the $\hat{z}$ axis unless the elastic constants are the same. Note that this invariance is also broken by the presence of the magnetic field but not by the presence of the electrical field. A direct consequence of this term is that is that B-L walls which are neither parallel nor perpendicular to the magnetic field (mixed wall) have a non-zero n_y component proportional to $K_1 - K_2$. This fact is confirmed by our numerical simulation.

We now investigate the effect of the curvature on the Ising-Bloch transition. We follow the experimental procedure described in 3.1.2. We start with a circular B-L walls and slowly increase the electrical field. We observed numerically that the Ising wall looses stability towards a state composed of four vortices joining four Bloch-walls (Fig. 4). This effect can be analytically investigated by making the following assumption. The radius r_0 of the B-L wall should be large enough so that we neglect the shrinkage velocity, but small enough so that the curvature effect can overcome the random effect of thermal fluctuation. In this limit, a simple analysis of equation (4) shows that X reads

$$X = \sqrt{\mu+\gamma}\tanh((r-r_0)(\sqrt{\frac{\mu+\gamma}{2K_2}})). \quad (5)$$

The Y component, which is adiabatically slaved to X, reads:

$$Y \sim (K_1-K_2)X_{xy} \sim \sin(2\varphi)(X'' - X'/r_0) \quad (6)$$

φ is the polar angle of the (x,y) plane, $r^2 = x^2+y^2$ and the primes represent derivatives with respect to r.

The term in X'' shows that a mixed wall has a double bump in Y while the last term proportional to the curvature has a single bump. As a consequence this dependence on the polar angle anticipates the formation vortices at the four cardinal points defined by $\sin(2\varphi) = 0$ when crossing the Ising-Bloch bifurcation.

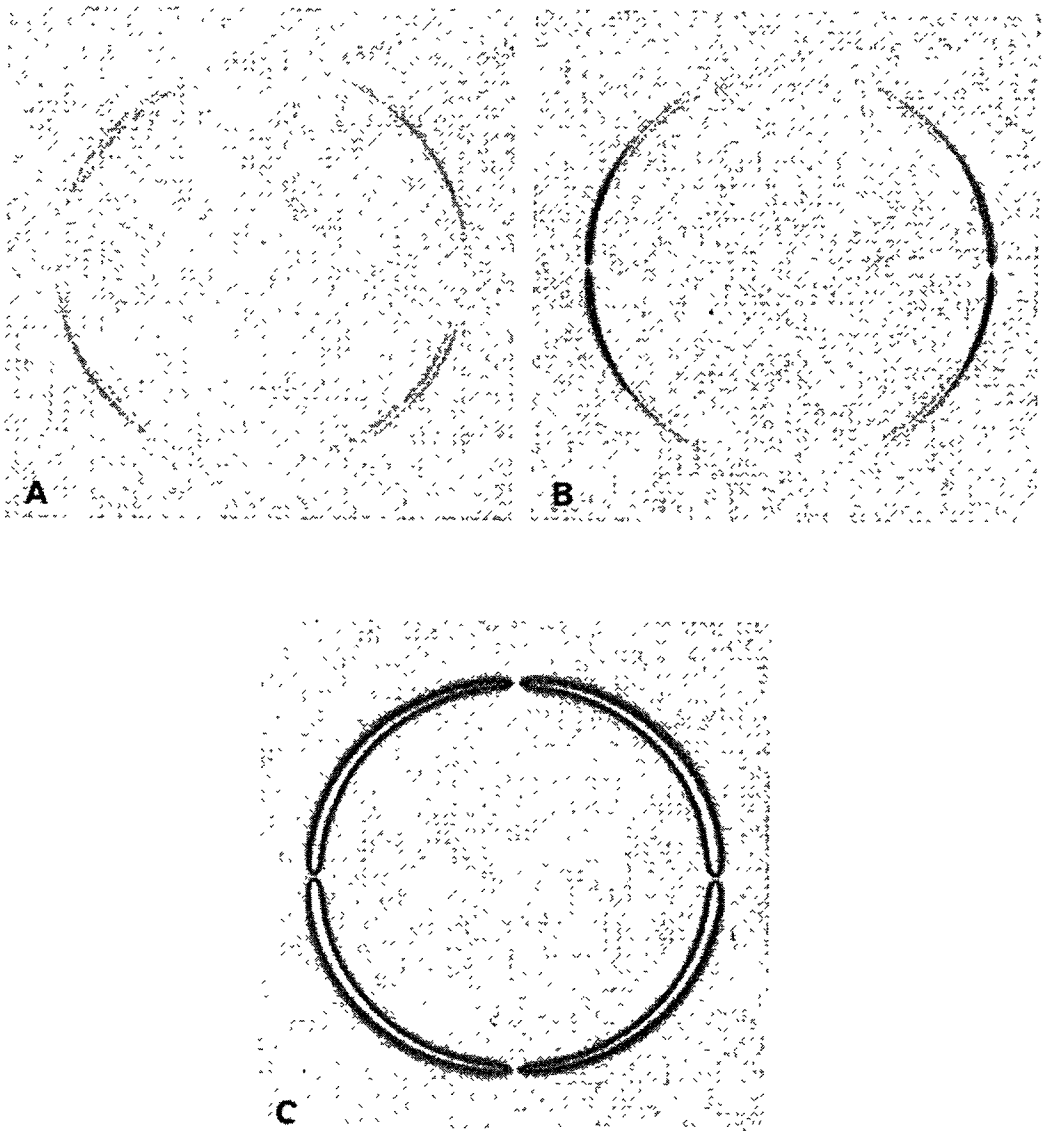

Fig. 4. — The numerical simulation of the G-L equation with $\omega = 0$: the dark regions correspond to a non-zero value of n_y a) in the Ising domain of the (H^2, E^2) parameter space, the asymmetry of n_y is clearly seen, n_y being stronger in the outer part of the ring. b) When $E_2 > E > E_1$, the formation of two -1 defects is observable in the horizontal region, parallel to H, c) the Bloch ring with four defects obtained for $E > E_2$.

5. Discussion.

In the $\omega = 0$ case, and in the (V^2, H^2) theoretical phase diagram (Fig. 2), two straight lines passing by the $H = 0$, $V_c = \pi(K_3/\epsilon_a)^{1/2}$ point (the threshold of the electrical Freedericksz transition) correspond to the onset of the I-B transition which is different for the two kinds of

B-L wall (either perpendicular or parallel to the magnetic field). In our experimental situation which produces the spontaneous straight wall, we consider the perpendicular case and the preliminary measurements shown in figure 2 demonstrate a satisfactory agreement with the model. The I-B transition threshold of the Splay-Bend B-L wall is linear in the (V^2, H^2) parameter space and the slope difference can be explained by uncertainties in the value of the elastic anisotropy of our samples.

The situation of the looped wall can also be understood within the framework of this model and figure 4 shows the simulation of the G-L equation for an increasing voltage in the presence of a magnetic field along the $\hat{x}$ axis. It demonstrates a behavior very close to the previously described experiment: -1 defects first appear along the H direction, followed at higher voltage by the localization of the $+1$ defects in the perpendicular direction. Moreover, pretransitional numerical phenomena are observed in the intermediate curved regions of the loop, before the non singular defects appear. Using the classical nail convention, the experimental and numerical observations are explained in figure 3. We first consider the idealized structure of a straight B-L wall, tilted by $\pi/4$ relative to the pure splay-bend or twist wall represented in figure 3a. In this case, corresponding to the isotropic elasticity case ($K_1 = K_2 = K_3$), the director projection n_y remains equal to zero when crossing the wall. In the real case, as seen from the colors experimentally observed when interposing a waveplate after the analyzer of the microscope, and also from the numerical model, the anisotropy of elastic constants, which is present in the common nematic situation, strongly favors the twist deformation, and, coming from the anisotropic coupling term, X_{xy}, in equation (3), spontaneously appears, as seen in figure 3b. The n_y component awakes with a sign inversion in the core of the wall where $n_x = n_y = 0$. We see that in this case the I-B transition has to choose arbitrarily (Fig. 3c) between both possible and equivalent tilt directions ($n_y < 0$ or $n_y > 0$), which makes the disclination trapping possible.

If we now focus our attention on the rounded loop of figure 3d, the curvature of the intermediate regions introduces a remarkable modification of this situation. The variation of the n_y component is no longer symmetric relative to the wall, and the external region of the loop gives rise to a stronger deviation which suppresses the degeneracy of the I-B transition and determines the tilting direction of n. As the threshold value for the I-B transition is lower in the splay-bend region, and since the director tilting direction is reversed in successive quadrants of figures 3d, e, two -1 defects with $n_x = n_y = 0$ in their core remain trapped in the horizontal region of the loop. In a following step, two $+1$ are localized in the initially pure twist vertical region, when the threshold value of the twist I-B transition is reached.

6. Conclusion.

We have experimentally investigated the Ising-Bloch transition in a nematic liquid crystal. The transition is second order and induces a change in the nature of the walls observed in the experiment. Furthermore we have developed a theoretical model which is in good quantitative agreement with our experimental observation of the Ising-Bloch transition. In the out-of-equilibrium case, corresponding to reference [1], an experiment which we have reproduced, we have also observed the formation of rotating spirals, with different pitches associated with the -1 or $+1$ defects. Moreover, interesting details concerning the looped wall transformation, which is more complex in this out-of-equilibrium case, will be described in reference [3].

In the future, the influence of the elastic anisotropy will be investigated close to the Smectic A-Nematic transition. The influence of the chirality will also be investigated experimentally and theoretically.

Acknowledgments.

The authors would like to thank S. Rica and P. Coullet for their contribution to the theoretical part of this work, Dr Velicesco from the company Vac, Germany, for kindly providing the high flux permanent magnets and Lois Hoffer for numerous suggestions.

References

[1] a)Migler K. B., PhD Thesis, Brandeis University, Boston, USA (1991);
b) Migler K. B., Meyer R. B., *Phys. Rev. Lett.* **66** (1991) 1485.

[2] Brochard F., Leger L., Meyer R. B., *J. Phys. France* **36** (1975) C1-209.

[3] Frisch T., Rica S., Coullet P., Gilli J. M., Spiral waves in liquid crystal, submited to *Phys. Rev. Lett.* (September 1993).

[4] Coullet P., Lega J., Houchmanzadeh B., Lajzerowicz J., *Phys. Rev. Lett.* **65** (1990) 1352;
Coullet P., Lega J., Pomeau Y., *Europhys. Lett.* **15** (1991) 221.

[5] Leger L., *Solid State Commun.* **11** (1972) 1499; *Mol. Cryst. Liq. Cryst.* **24** (1973) 33; Thèse d'état, Université Paris Sud, Orsay, France (1976).

[6] Bulaevskii L. N., Ginzburg V. L., *Zh. Eksp. Teor. Fiz.* **45** (1963) 772; *Sov. Phys. JETP* **18** (1964) 530.

[7] Lajzerowicz J., Niez J. J., *J. Phys. France Lett.* **40** (1979) L-165.

[8] de Jeu W. H., Claassen W. A. P., Spruijt A. M. J., *Mol. Cryst. Liq. Cryst.* **37** (1976) 269.

[9] a) Gilli J. M., Morabito M.; b) Coullet P., Proceedings of the Workshop From excitability to oscillations - a case study in spatially extended systems, Nice (June 2-5, 1993).

[10] Vidal C., Pacault A., Nonlinear Phenomena in Chemical Dynamics (Springer-Verlag, Heidelberg, 1981).

[11] Devreotes P. N., *Adv. Cycl. Nucl. Res.* **15** (1983) 55.

[12] Lonberg F., Meyer R. B., *Phys. Rev. Lett.* **55** (1985) 718;
Hurd A. J., Fraden S., Lonberg F., Meyer R. B., *J. Phys. France* **46** (1985) 905.